Supporting Information

Yin et al. 10.1073/pnas.1215928109

SI Materials and Methods

Baculovirus DR52c–Peptide Libraries. The baculovirus libraries described in Fig. 1 were produced by direct cloning of PCR fragments into baculovirus DNA (1, 2). The baculovirus DNA was digested with homing nucleases SceI and CeuI, leaving 3′ overhanging ends. The PCR fragment encoding the randomized peptide library was digested with homing nucleases BstXI and purified. The mixture of digested baculovirus DNA and the digested PCR fragment was ligated with a high concentration of T4 ligase (10^5 units/mL) for 1 h at room temperature. The ligation mixture was heated, inactivated, and directly used for transfecting SF9 insect cells using the standard calcium phosphate method. The transfected SF9 insect cells were then sorted by Alexa Fluor647-labeled ANi2.3 T-cell receptor (TCR) multimers 3 d later.

T Cells and T-Cell Assays. The activation of ANi2.3 T-cell transfectoma (3, 4) or its mutational variants was assayed by IL-2 secretion as previously described (5). Mutant variants of ANi2.3 were made by retroviral transduction of the TCR^- T-cell hybridoma 5KC-9c6 (6, 7). Three types of antigen-presenting cells were used: (*i*) ICAM/B7.1$^+$ SF9 insect cells (1) infected with baculovirus encoding a surface-expressed version of DR52c bearing a linked DR52c binding peptide (2); (*ii*) DR52c$^+$ HO301 lymphoblastoid B cells (8); and (*iii*) DT40 chicken leukemia B cells (9) transduced with retroviruses encoding DR52c linked to the pHIR mimotope.

TCR Mutational Analysis. Wild-type and the indicated alanine-substitution mutants of ANi2.3 Vα and Vβ were cloned in murine stem cell virus (MSCV)-based retroviral plasmids with an internal ribosomal entry site plus green fluorescent protein as a reporter. TCR chains were expressed in TCR-deficient human CD4-transduced hybridoma cell line 5KC-9c6 (6) by retroviral transduction as described previously (10, 11). Cells expressing equivalent levels of TCR and CD4 were isolated by flow cytometry cell sorting. Ten thousand cells of each mutant transfectoma were used for the T-cell assays.

Protein Expression and Purification. DNA encoding DR52c (extracellular domains) and DR52c β-chain covalently attached to pHIR or pWIR was cloned into a single baculovirus as previously described (12). The soluble DR52c–pHIR and DR52c–pWIR complexes in the supernatants of virus-infected HighFive insect cells were purified by immunoaffinity chromatography using the anti-DR mAb LB-3.1, followed by size-exclusion chromatography using Superdex 200. For Biacore surface plasmon resonance experiments, V regions of the ANi2.3 TCR were fused to mouse C regions and expressed in baculoviruses as previously described (13–15). For crystallography, the Vα and Vβ portions of the ANi2.3 TCR were fused by GS linker (Vα-linker-Vβ) in a modified (Fig. S1) version of the Mopac16 vector (16). The soluble single-chain ANi2.3 TCR was expressed in the periplasmic space of the Rosetta strain of *Escherichia coli* and purified by an Ni-NTA affinity column and a Superdex 200 gel-filtration column.

Crystal Production and Data Collection. DR52c–pHIR and DR52c–pWIR were crystallized by mixing 0.5 μL of each protein solution at a concentration of 15 mg/mL with an equal volume of reservoir solution. DR52c–pHIR was crystallized in 16% PEG 4000, 100 mM Tris·HCl (pH 8.0) with space group C2. DR52c–pWIR was crystallized in 17% PEG 4000, 100 mM HEPES (pH 7.5), 10% isopropanol with space group $P2_1$. An equimolar mixture of ANi2.3 TCR and DR52c–pHIR was crystallized by mixing 0.5 μL of complex solution at a concentration of 15 mg/mL with an equal volume of reservoir solution. The complex was crystallized in 12% PEG 3350, 100 mM ammonium tartrate (pH 7.0) in space group $P6_3$.

Data Collection. X-ray diffraction data were collected at the Advanced Light Source on beamline 8.2.2 under liquid-nitrogen cryoconditions at 100 K. All crystals were flash-cooled in liquid nitrogen after a flash-soak in a cryoprotection solution consisting of the reservoir solution with an additional concentration of glycerol (18–25%). The data were indexed, integrated, scaled, and merged using HKL2000 (17).

Structure Determination. The structures of DR52c–pHIR and DR52c–pWIR were determined by molecular replacement using the CCP4 program AMoRe (18) with the DR52c–pTu structure [Protein Data Bank (PDB) ID code 3C5J] without a bound peptide as the search model. In the initial $F_o - F_c$ maps, we could see a clear positive density within the peptide binding groove of DR52c. Peptides were modeled into this positive density. Models were manually adjusted using the program O (19).

The structures of the ANi2.3–DR52c–pHIR complex were determined by molecular replacement using Phaser (20) with the Vα of HA1.7 TCR (PDB ID code 1FYT), Vβ of JM22 TCR (PDB ID code 1OGA), and DR52c–pTu (PDB ID code 3C5J) as search models, respectively. After an initial round of rigid-body refinement, the models were inspected and manually fitted with the program Coot (http://lmb.bioch.ox.ac.uk/coot). The models were then subjected to several rounds of alternating simulated annealing/positional refinement in PHENIX (21) followed by B-factor refinement in PHENIX. Model building was performed using the program Coot from the CCP4 suite. Simulated annealing omit maps were routinely used to remove the model bias. All models have good stereochemistry, as determined by the program PROCHECK (22).

Structure Analysis. Buried molecular surface areas were calculated using GRASP (23). NCONT in CCP4 (18) was used to analyze the contacts between the TCRs and their ligands. Atoms within 4.5 Å of each other were considered part of the interface. Contacts involving potential electron donors and acceptors (O or N) within 3.5 Å were considered potential hydrogen bonds or salt bridges. Other contacts were considered van der Waals contacts. Molecular superimpositions and figures were created with PyMOL (Schrödinger) and Swiss-PDB Viewer (24).

1. Crawford F, Huseby E, White J, Marrack P, Kappler JW (2004) Mimotopes for alloreactive and conventional T cells in a peptide-MHC display library. *PLoS Biol* 2(4): E90.
2. Crawford F, et al. (2006) Use of baculovirus MHC/peptide display libraries to characterize T-cell receptor ligands. *Immunol Rev* 210:156–170.
3. Lu L, et al. (2003) Components of the ligand for a Ni^{++} reactive human T cell clone. *J Exp Med* 197(5):567–574.
4. Vollmer J, Fritz M, Dormoy A, Weltzien HU, Moulon C (1997) Dominance of the BV17 element in nickel-specific human T cell receptors relates to severity of contact sensitivity. *Eur J Immunol* 27(8):1865–1874.
5. White J, Kappler J, Marrack P (2000) Production and characterization of T cell hybridomas. *Methods Mol Biol* 134:185–193.
6. White J, Pullen A, Choi K, Marrack P, Kappler JW (1993) Antigen recognition properties of mutant Vβ3$^+$ T cell receptors are consistent with an immunoglobulin-like structure for the receptor. *J Exp Med* 177(1):119–125.
7. Bowerman NA, Falta MT, Mack DG, Kappler JW, Fontenot AP (2011) Mutagenesis of beryllium-specific TCRs suggests an unusual binding topology for antigen recognition. *J Immunol* 187(7):3694–3703.
8. Yang SYE, Milford E, Hammerling U, Dupont B (1989) Description of the reference panel of B-lymphoblastoid cell lines for factors of the HLA system: The B cell panel

designed for the Tenth International Histocompatibility Workshop. *Immunobiology of HLA*, ed Dupont B (Springer, New York), pp 11–19.
9. Baba TW, Giroir BP, Humphries EH (1985) Cell lines derived from avian lymphomas exhibit two distinct phenotypes. *Virology* 144(1):139–151.
10. Rubtsova K, et al. (2009) Many different Vβ CDR3s can reveal the inherent MHC reactivity of germline-encoded TCR V regions. *Proc Natl Acad Sci USA* 106(19):7951–7956.
11. Scott-Browne JP, et al. (2007) Germline-encoded recognition of diverse glycolipids by natural killer T cells. *Nat Immunol* 8(10):1105–1113.
12. Dai S, Crawford F, Marrack P, Kappler JW (2008) The structure of HLA-DR52c: Comparison to other HLA-DRB3 alleles. *Proc Natl Acad Sci USA* 105(33):11893–11897.
13. Huseby ES, et al. (2005) How the T cell repertoire becomes peptide and MHC specific. *Cell* 122(2):247–260.
14. Kappler J, White J, Kozono H, Clements J, Marrack P (1994) Binding of a soluble αβ T-cell receptor to superantigen/major histocompatibility complex ligands. *Proc Natl Acad Sci USA* 91(18):8462–8466.
15. Veien NK (2011) Systemic contact dermatitis. *Int J Dermatol* 50(12):1445–1456.
16. Maynard J, et al. (2005) High-level bacterial secretion of single-chain αβ T-cell receptors. *J Immunol Methods* 306(1-2):51–67.
17. Otwinowski Z, Minor W (1997) Processing of X-ray diffraction data collected in oscillation mode. *Macromolecular Crystallography Part A*. Methods in Enzymology, eds Carter CW, Jr, Sweet RM (Academic, New York), Vol. 276, pp 307–326.
18. Collaborative Computational Project, Number 4 (1994) The CCP4 suite: Programs for protein crystallography. *Acta Crystallogr D Biol Crystallogr* 50(Pt 5):760–763.
19. Jones TA, Zou JY, Cowan SW, Kjeldgaard M (1991) Improved methods for building protein models in electron density maps and the location of errors in these models. *Acta Crystallogr A* 47(Pt 2):110–119.
20. McCoy AJ, et al. (2007) Phaser crystallographic software. *J Appl Crystallogr* 40(Pt 4): 658–674.
21. Adams PD, et al. (2002) PHENIX: Building new software for automated crystallographic structure determination. *Acta Crystallogr D Biol Crystallogr* 58(Pt 11):1948–1954.
22. Laskowski RA, MacArthur DS, Moss DS, Thornton JM (1993) PROCHECK: A program to check the stereochemical quality of protein structures. *J Appl Crystallogr* 26(Pt 2):283–291.
23. Nicholls A, Sharp KA, Honig B (1991) Protein folding and association: Insights from the interfacial and thermodynamic properties of hydrocarbons. *Proteins* 11(4):281–296.
24. Kaplan W, Littlejohn TG (2001) Swiss-PDB Viewer (Deep View). *Brief Bioinform* 2(2): 195–197.

Modified portion of Mopac54:

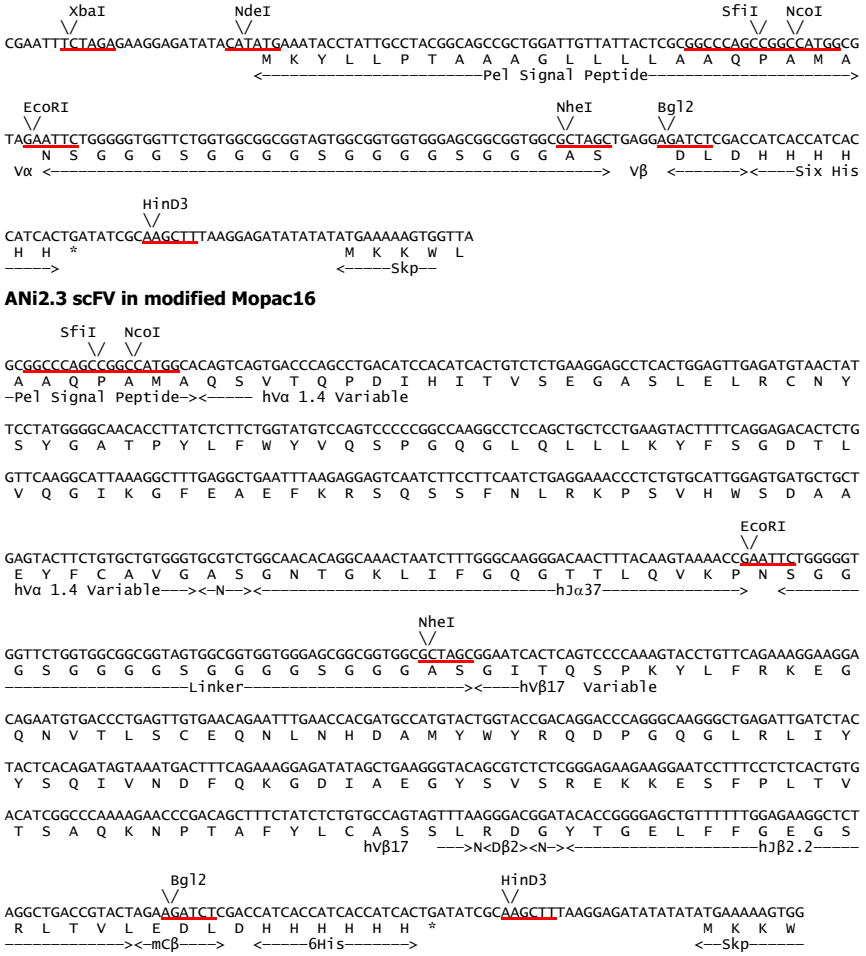

Fig. S1. Modification of pMopac54 and cloning of the ANi2.3 TCR as a single-chain Fv (scFV). The original Mopac54 plasmid was modified to introduce cloning sites for TCR Vα (NcoI and EcoRI) before and Vβ (NheI and Bgl2) after the GS linker. Also, the sequence encoding human Cκ and residual *E. coli* phage sequence (~500 bp) was removed between the scFV and Skp gene, the original 12-His tag was reduced to a 6-His tag, and an out-of-frame ATG in the Pel signal peptide was removed by changing codon 3 from TGC to TAC. DNA fragments encoding the Vα and Vβ domains of ANi2.3 flanked by the appropriate restrictions sites were synthesized by PCR and cloned into the modified vector.

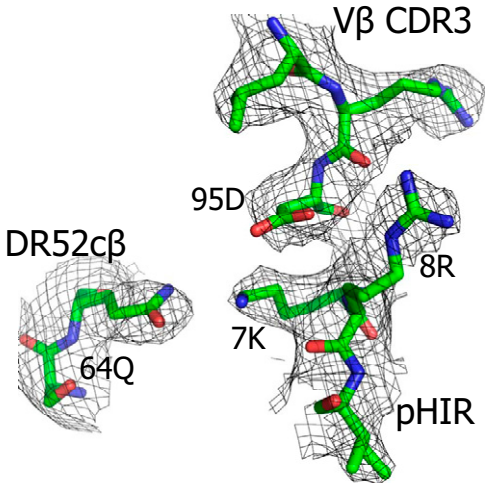

Fig. S2. Electron density at the interface among DR52c, TCR Vβ CDR3, and pHIR. A section of the ANi2.3 TCR Vβ CDR3 loop, the alpha helix of DR52c β1 domain, and the C-terminal end of the pHIR mimotope are shown with electron density based on the final model (2Fo-Fc, 1.5σ). The side chains of the critical TCR βCDR3β D95, DR52c β1 Q64, and pHIR 7K and 8R are labeled.

Other Supporting Information Files

Table S1 (DOC)
Table S2 (DOC)
Table S3 (DOC)
Table S4 (DOC)
Table S5 (DOC)